J. Biochem. 2012;152(2):199–206 doi:10.1093/jb/mvs068

JB THE JOURNAL OF BIOCHEMISTRY

A mechanistic study of the formation of hydroxyl radicals induced by horseradish peroxidase with NADH

Received February 2, 2012; accepted April 27, 2012; published online June 19, 2012

Toshiaki Miura*

Department of Biology in Hokkaido Pharmaceutical University School of Pharmacy, Katsuraoka-cho7-1, Otaru, 0470264 Japan

*Tel: +81-134-62-5111, Fax: +81-134-62-5161, email: miurat@hokuyakudai.ac.jp

During the oxidation of NADH by horseradish peroxidase (HRP-Fe^{3+}), superoxide (O_2^-) is produced, and HRP-Fe^{3+} is converted to compound III. Superoxide dismutase inhibited both the generation of O_2^- and the formation of compound III. In contrast, catalase inhibited only the generation of O_2^-. Under anaerobic conditions, the formation of compound III did not occur in the presence of NADH, thus indicating that compound III is produced via formation of a ternary complex consisting of HRP-Fe^{3+}, NADH and oxygen. The generation of hydroxyl radicals was dependent upon O_2^- and H_2O_2 produced by HRP-Fe^{3+}-NADH. The reaction of compound III with H_2O_2 caused the formation of compound II without generation of hydroxyl radicals. Only HRP-Fe^{3+}-NADH (but not $K^+O_2^-$ and xanthine oxidase-hypoxanthine) was able to induce the conversion of metmyoglobin to oxymyoglobin, thus suggesting the participation of a ternary complex made up of HRP-$Fe^{2+}\cdots O_2\cdots NAD^{\cdot}$ (but not free O_2^- or H_2O_2) in the conversion of metmyoglobin to oxymyoglobin. It appears that a cyclic pathway is formed between HRP-Fe^{3+}, compound III and compound II in the presence of NADH under aerobic conditions, and a ternary complex plays the central roles in the generation of O_2^- and hydroxyl radicals.

Keywords: compound III/hydroxyl radical/NAD radical/peroxidase/superoxide.

Abbreviations: DTPA, diethylenetriaminepentaacetic acid; ESR, electron spin resonance; HRP, horseradish peroxidase; HX, hypoxanthine; Mb, myoglobin; POBN, α-(4-pyridyl-*N*-oxide)-*N*-tert-butylnitrone; SOD, superoxide dismutase; XO, xanthine oxidase.

It is believed that peroxidases protect cells from the destructive influence of H_2O_2 or its derived oxygen species (*1*). In the presence of H_2O_2, peroxidase catalyzes single electron oxidation through the catalytic cycle as follows (*2*, *3*).

$$\text{Peroxidase (ferricperoxidase)} + H_2O_2 \rightarrow \text{Compound I} + H_2O$$

$$\text{Compound I} + AH_2 \rightarrow AH\cdot + \text{Compound II}$$

$$\text{Compound II} + AH_2 \rightarrow AH\cdot + \text{Ferricperoxidase} + H_2O$$

$$2AH\cdot \rightarrow A + AH_2$$

Compound I and II are powerful oxidants that can cause the oxidation of various substrates.

Alternatively, peroxidases also exhibit an oxidase activity that mediates the reduction of oxygen to superoxide (O_2^-) and H_2O_2 through the formation of compound III in the presence of NADH (*4*–*7*). During the formation of compound III, hydroxyl radicals ($HO^{\cdot}$), which are highly reactive molecules capable of degrading numerous cellular components, are produced from the reaction of O_2^- and H_2O_2 (*8*–*10*). Schopfer and colleagues (*11*–*13*) suggest that ferric and perferryl peroxidases constitute effective biochemical catalysts for production of $HO^{\cdot}$ from H_2O_2, thus speculating that compound III can act like a Fenton reagent.

On the other hand, Fujimoto *et al*. (*14*–*16*) showed that myeloperoxidase efficiently catalyzes the hydroxylation of phenylalanine to tyrosine in the presence of NADH. They proposed that hydroxyl radicals are produced through a non–iron-catalyzed mechanism. Therefore, the precise mechanism(s) by which $HO^{\cdot}$ is generated by the oxidase activity of peroxidase in the presence of NADH remains to be determined.

Phagocytic cells such as neutrophils and macrophages participate in inflammation and the host defense against microbial challenge (*17*). The activated phagocytic cells are drawn to the site of injury, while secreting superoxide generated through the action of a membrane-associated NADPH-dependent oxidase (*18*, *19*). The superoxide then dismutates into hydrogen peroxide. It is generally recognized that the reaction of O_2^- with H_2O_2 produces $HO^{\cdot}$ via the iron-catalyzed Haber–Weiss reaction (*20*, *21*). As such, hydroxyl radicals participate in the bactericidal activity and the pathology of tissue injury induced by phagocytic cells (*22*–*26*). However, it is unclear whether the formation of compound III contributes to the generation of $HO^{\cdot}$ to play a role in either the bactericidal activity or tissue injury induced by phagocytic cells.

The present study suggests that a cyclic pathway is formed among HRP-Fe^{3+}, compound III and compound II in the presence of NADH under aerobic

conditions, and a ternary complex indicated as HRP-$Fe^{2+}\cdots O_2\cdots NAD^{\cdot}$ but not NAD radical plays a central role in the generation of O_2^- and $HO^{\cdot}$.

Materials and Methods

Materials

HRP-Fe^{3+} and NADH were obtained from the Oriental Yeast Co. (Tokyo, Japan); hypoxanthine (HX) and diethylenetriaminepentaacetic acid (DTPA) were from Wako Pure Chemical Industry (Osaka, Japan); cytochrome *c* (horse heart), myoglobin (Mb, equine heart), superoxide dismutase (SOD, bovine liver) and α-(4-pyridyl-*N*-oxide)-*N*-tert-butylnitrone (POBN) were from Sigma Chemical Co. (St. Louis, MO, USA). The potassium superoxide ($K^+O_2^-$) was from Strem Chemicals, Co. (Newburyport, MA, USA); xanthine oxidase (XO) was from Biozyme Laboratories Ltd. (Gwent, UK). All other chemicals were analytical grade products obtained from commercial suppliers. To remove traces of iron, the buffers used in this study were treated with chelex 100.

Enzyme activity assays

The HRP-Fe^{3+} concentration was determined spectrophotometrically ($\varepsilon_{402} = 1.02 \times 10^5\,M^{-1}\,cm^{-1}$) (*27*). The ratio of the absorbance at 402 nm to that at 280 nm of the enzyme (Rz value) was 3.0. The activity of HRP-Fe^{3+} was measured by using the method reported by Das *et al*. (*28*). XO was dialyzed against 10 mM phosphate buffer pH 7.4 before use. The enzyme activity was determined by measurement of the conversion of HX to uric acid at 293 nm (*29*). One unit of XO was defined as that which formed 1.0 μM uric acid /min at pH 7.4.

Measurement of superoxide production

The generation of superoxide was determined by measuring the reduction of cytochrome *c* at 550 nm (*30*). The reaction mixture contained 2.5 μM HRP-Fe^{3+}, 1.0 mM NADH and 30 μM cytochrome *c* ($\varepsilon_{550} = 2.78 \times 10^2\,cm^{-1}$) in 50 mM acetate buffer pH 6.0 containing 0.1 mM DTPA.

Electron spin resonance (ESR)

The ESR signal of $HO^{\cdot}$ was measured by the method previously reported by Ramos *et al*. (*31*). The reaction mixture contained 1.3 μM HRP-Fe^{3+}, 170 mM ethanol, 10 mM POBN and 0.5 mM NADH in 50 mM acetate buffer containing 0.1 mM DTPA. The ESR spectra of the hydroxyethyl-POBN adduct formed were recorded at room temperature in a flat cell. The ESR setting was as follows: microwave power, 10 mW; modulation frequency, 100 kHz; modulation field, 0.1 G; receiver gain, 1000 and time constant, 0.3 s.

Reaction of HRP-Fe^{3+} with NADH

The formation of compounds I, II and III from HRP-Fe^{3+} was analysed spectrophotometrically (*6*). The reaction mixtures were consisted of 10 μM HRP-Fe^{3+} and 0.5 mM NADH in 50 mM acetate buffer pH 6.0 containing 0.1 mM DTPA. $K^+O_2^-$ was diluted with NaCl in a mortar. Powdered $K^+O_2^-$ was added to the reaction mixture. The XO-HX system consisted of 0.025 u/ml XO and 0.1 mM hypoxanthine (HX) in 50 mM acetate buffer (pH 6.0) containing 0.1 mM DTPA.

Results

Formation of superoxide

As shown in Fig. 1, O_2^- was generated during the reaction of HRP-Fe^{3+} with NADH (HRP-Fe^{3+}-NADH) under aerobic conditions. Superoxide was detected by the reduction of cytochrome *c*. When HRP-Fe^{3+} or NADH was omitted from the reaction mixture, no generation of O_2^- was observed. The insert in Fig. 1 shows the double reciprocal plots of NADH oxidized by HRP-Fe^{3+}. The Km value of HRP-Fe^{3+} to NADH was 1.0 mM. Fig. 2 shows the inhibitory effect of SOD and catalase on the reduction of cytochrome *c*. SOD scavenged O_2^-, and catalase strongly inhibited the generation of O_2^- in a concentration-dependent manner.

Formation of compound III

Fig. 3A shows the formation of compound III from HRP-Fe^{3+} in the presence of NADH. Compound III, which has two characteristic peaks at 546 and 580 nm, was formed during the reaction of HRP-Fe^{3+} with NADH under aerobic conditions. SOD strongly inhibited this process, whereas catalase promoted the formation of compound III. When HRP-Fe^{3+} was incubated with NADH under anaerobic conditions, there was minimal conversion of HRP-Fe^{3+} to compound III. These results suggest that compound III was formed through a ternary complex consisting of HRP-Fe^{3+}, NADH and oxygen, rather than the reaction of ferroperoxidase with O_2.

It was previously assumed that HRP-Fe^{3+} directly reacts with O_2^- generated by the radio pulse technique

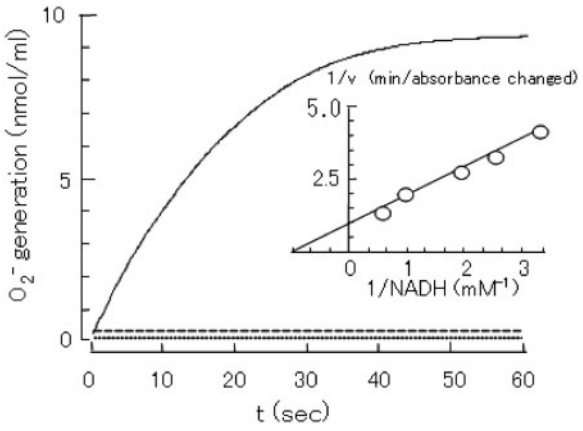

Fig. 1 The generation of O_2^- induced during the reaction of HRP-Fe^{3+} with NADH. The reaction mixture consisted of HRP-Fe^{3+} (2.5 μM), NADH (1.0 mM) and cytochrome *c* (30 μM) in 50 mM acetate buffer pH 6.0 containing DTPA (0.1 mM). The generation of O_2^- was continuously monitored by measuring the reduction of cytochrome *c* at 550 nm. The reaction was started by addition of HRP-Fe^{3+}. Solid, dotted and broken lines indicate the complete reaction mixture, without NADH and without HRP-Fe^{3+}, respectively. In insert, conditions were the same as in Fig.1, with the exception of the concentrations of NADH. Each point represents the mean of triplicate experiments.

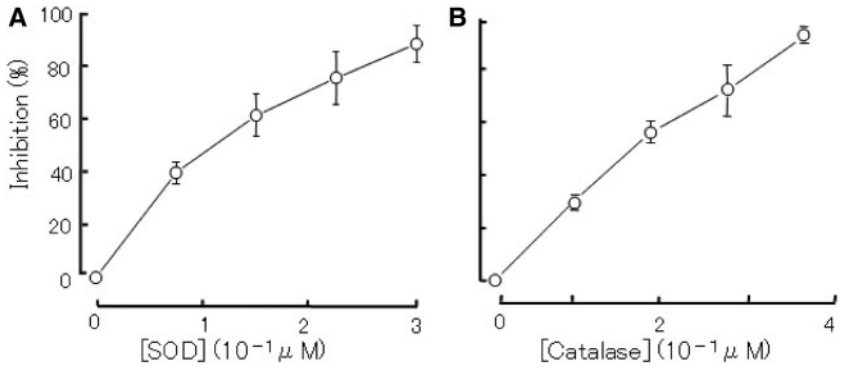

Fig. 2 Inhibitory effects of SOD (A) and catalase (B) on the generation of O_2^- from HRP-Fe^{3+}-NADH. Conditions were the same as described in Fig. 1 except for the addition of different concentrations of SOD and catalase. Each value represents the mean ± standard deviations of five experiments.

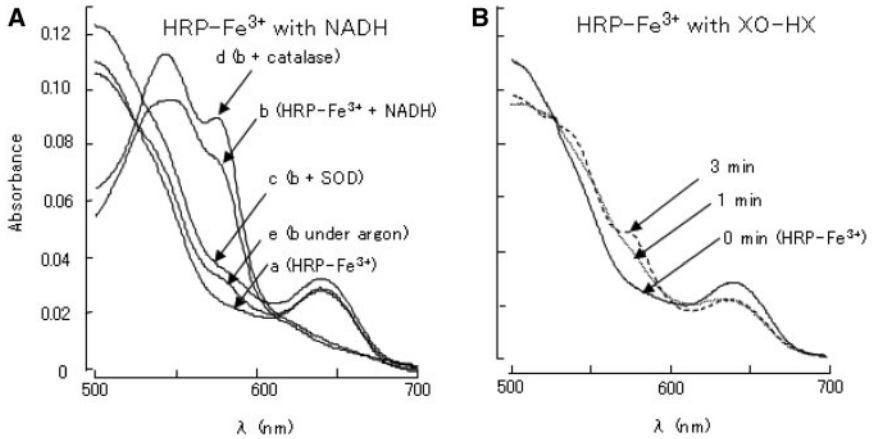

Fig. 3 Formation of compound III during the reaction of HRP-Fe^{3+} with NADH (A) or XO-HX (B). (A) The reaction mixture contained HRP-Fe^{3+} (10 μM) and NADH in 50 mM acetate buffer (pH 6.0) containing DTPA (0.1 mM). The reaction was started by addition of NADH (1.0 mM). SOD (3 μM) and catalase (0.4 μM) were added to the reaction mixture before the start of the reaction. The spectra were recorded at 1 min after the start of the reaction. For anaerobic conditions, the solutions of HRP-Fe^{3+} and NADH were purged with argon gas for 10 min and then the reaction was started by adding NADH to the solution of HRP-Fe^{3+}. Curve a, HRP-Fe^{3+}; curve b, HRP-Fe^{3+}-NADH; curve c, curve b + SOD; curve d, curve b + catalase; and curve e, curve b under anaerobic conditions. (B) The reaction mixture contained HRP-Fe^{3+} (10 μM), XO (0.025 u/ml), HX (0.1 mM), catalase (0.8 μM) in 50 mM acetate buffer (pH 6.0) containing DTPA (0.1 mM). The reaction was started by adding XO. The spectra were recorded at 0 (solid line), 1 (dotted line) and 3 (broken line) min.

to produce compound III (*32*, *33*). Fig. 3B shows the formation of compound III from the reaction of HRP-Fe^{3+} with O_2^-. When HRP-Fe^{3+} was incubated with XO and HX in the presence of catalase, it gradually converted to compound III. About 40% of HRP-Fe^{3+} was converted to the compound III at 3 min. Over 3 min, the compound III slightly decreased (data not shown). In the absence of catalase, the formation of compound III was not observed in the reaction system of XO-HX (data not shown).

Generation of the hydroxyl radical

Fig. 4A shows that $HO^{\cdot}$ was generated from HRP-Fe^{3+}-NADH. The triplet of doublets observed from the ESR, which corresponds to the hydroxyethyl-POBN adduct, occurred during the reaction of HRP-Fe^{3+} with NADH, in agreement with a previous report by Chen and Schopfer (*13*). The omission of NADH or HRP-Fe^{3+} led to loss of the ESR signal. SOD strongly inhibited the formation of $HO^{\cdot}$, and catalase completely inhibited its formation. Evidently, the formation of the hydroxyl radical is dependent upon both O_2^- and H_2O_2. Fig. 4B and C shows that the formation of $HO^{\cdot}$ was dependent upon the concentrations of HRP-Fe^{3+} and NADH. The relative intensities of the ESR signals of $HO^{\cdot}$ increased almost linearly up to 2.5 μM of HRP-Fe^{3+} and 0.8 mM of NADH, respectively. In addition, the ESR signals of the hydroxyethyl-POBN adduct did not occur during the reaction of $K^+O_2^-$ with H_2O_2 (data not shown). Furthermore, no decrease in the absorbance at 340 nm was observed during the incubation of NADH with $K^+O_2^-$ or H_2O_2, indicating that O_2^- and H_2O_2 did not directly oxidize NADH (data not shown). These results strongly suggest that the generation of $HO^{\cdot}$ was not due to a direct reaction of O_2^- with H_2O_2 produced from HRP-Fe^{3+}-NADH.

Involvement of compound III

I next examined whether $HO^{\cdot}$ was formed or not during the reaction of compound III with H_2O_2. As shown in Fig. 5A, addition of H_2O_2 caused a gradual

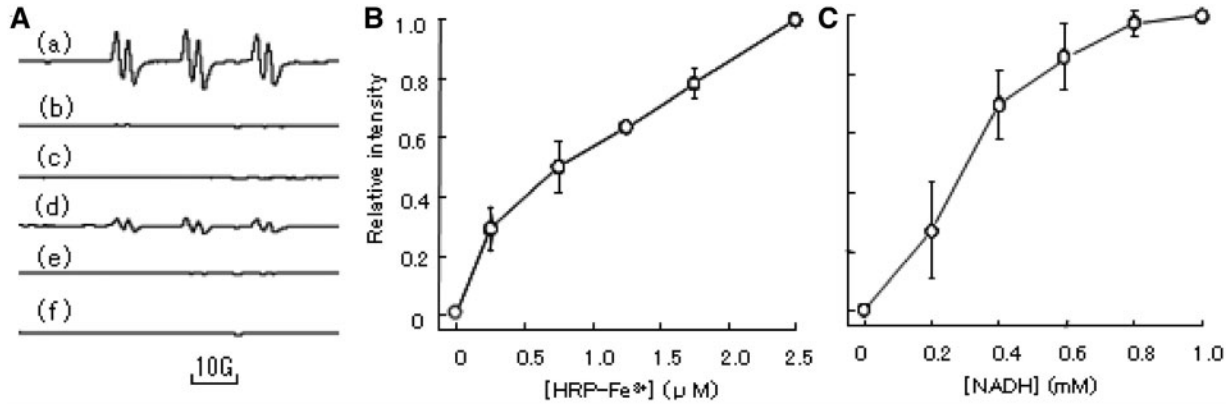

Fig. 4 Formation of $HO^{\cdot}$ during the reaction of HRP-Fe^{3+} with NADH (A) and the effect of concentrations of the HRP-Fe^{3+} (B) or NADH (C). (A) Conditions were described in the Methods section. a, complete; b, − HRP-Fe^{3+}; c, − NADH; d, + SOD (3 μM); e, + catalase (0.4 μM) and f, + SOD (3 μM) and catalase (0.4 μM). (B) and (C) Conditions were the same as described in (A) except for the concentrations of HRP-Fe^{3+} and NADH. Each point represents the means ± standard deviations of five experiments.

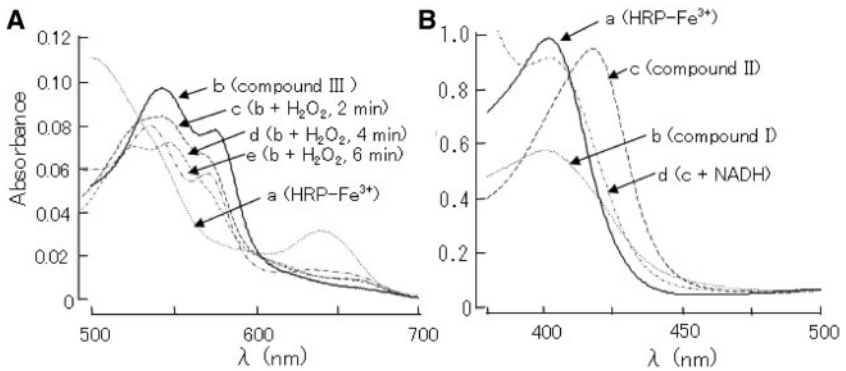

Fig. 5 Effect of H_2O_2 on the production of compound III induced by HRP-Fe^{3+}-NADH (A) and reduction of compound II by NADH (B). (A) The reaction mixture contained NADH (0.5 mM), HRP-Fe^{3+} (10 μM) and 0.1 mM DTPA in 50 mM acetate buffer pH 6 (a, dotted line). The spectrum of compound III (b, solid line) was recorded at 1 min after the addition of NADH. H_2O_2 (200 μM) was added to the reaction mixture. After 2 (c, broken line), 4 (d, one dotted solid line) or 6 (e, two dotted solid line) min, the spectra were recorded. (B) The spectrum of HRP-Fe^{3+} (10 μM) was recorded first at pH 7.0 of 50 mM phosphate buffer (a, solid line). An equimolar of H_2O_2 was then added to form compound I, and a scan was recorded (b, dotted line). After 30 s, an equimolar amount of potassium ferrocyanide was added to reduce compound I to compound II. The scan of compound II was recorded (c, broken line). Finally, NADH (0.5 mM) was added to the compound II. The reduction of compound II to HRP-Fe^{3+} was observed (d, single dotted solid line).

conversion of compound III to compound II. At 6 min after the start of the reaction, however, the spectrum of compound III was observed again. Fig. 5B shows that compound II was converted to HRP-Fe^{3+} by NADH. HRP-Fe^{3+} was in turn converted to compound I by an equivalent of H_2O_2, then ferrocyanide converted compound I to compound II. NADH led to conversion of compound II to HRP-Fe^{3+}. These results indicate that compound III was oxidized to compound II by H_2O_2, then compound II was reduced to HRP-Fe^{3+} by NADH. These reactions may be indicated as follows in equations (1) and (2):

$$\text{Compound III} + H_2O_2 \rightarrow \text{Compound II} + O_2 + H_2O \quad (1)$$

$$2\text{Compound II} + \text{NADH} + 4H^+ \rightarrow 2\text{HRP} - Fe^{3+} + 2H_2O + NAD^+ \quad (2)$$

Although data are not shown, when H_2O_2 was added to a reaction mixture consisting of HRP-Fe^{3+}-NADH, the intensity of the ESR signal was constant up to 0.1 mM of H_2O_2 and decreased at high concentrations of H_2O_2, indicating that H_2O_2 was not responsible for the enhancement of the ESR signal from HRP-Fe^{3+}-NADH.

Reduction of metmyoglobin

To obtain a better understanding of the formation of $HO^{\cdot}$, the generation of O_2^- by the different systems, HRP-Fe^{3+}-NADH, $K^+O_2^-$ and XO-HX, was observed using metMb. Fig. 6 shows the time course of formation of oxyMb induced by HRP-Fe^{3+}-NADH. When metMb was incubated with HRP-Fe^{3+}-NADH, it was gradually reduced to oxyMb, which has two characteristic peaks at 537 and 576 nm (*32*). The insert in the figure shows the change in the absorbance of oxyMb at 576 nm in either the presence or absence of HRP-Fe^{3+}. The formation of oxyMb was greatly enhanced by HRP-Fe^{3+}. Fig. 7 shows the effects of SOD and catalase on the formation of oxyMb. SOD and catalase strongly blocked the formation of oxyMb in a concentration-dependent manner.

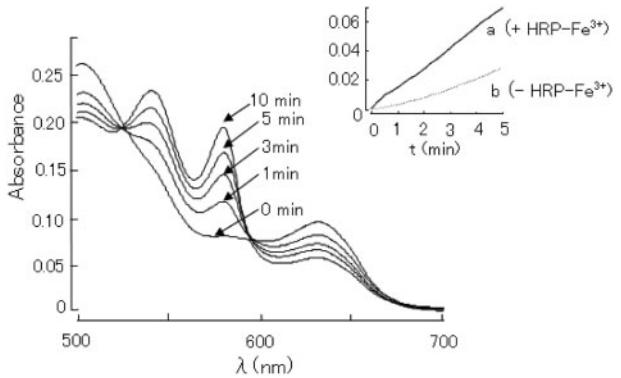

Fig. 6 Time course of the formation of oxyMb from metMb induced by HRP-Fe^{3+}-NADH. The reaction mixture contained HRP-Fe^{3+} (2.5 μM), NADH (1.0 mM) and metMb (30 μM). Other conditions were as described in Fig. 1. The reaction was started by addition of NADH. Numbers in the figure refer to the incubation time (min). After incubating, the spectra of Mb were recorded. The insert indicated a continuous increase in the absorbance at 576 nm in the presence (a, solid line) or absence (b, dotted line) of HRP-Fe^{3+}.

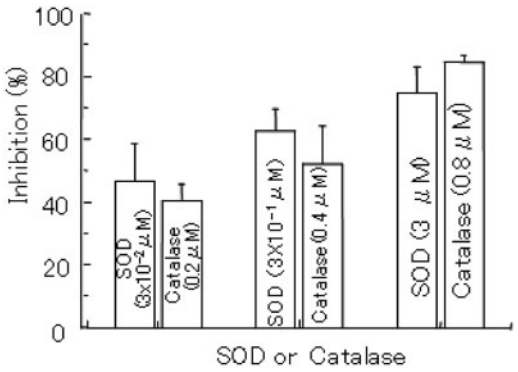

Fig. 7 Inhibitory effects of SOD and catalase on the formation of oxyMb. The conditions were the same as described in the insert (a) of Fig.6 except for the addition of SOD and catalase. The formation of oxyMb was measured by absorbance at 576 nm. Each value represents the mean ± standard deviations of five experiments.

In contrast, as shown in Fig. 8, neither $K^+O_2^-$ nor XO-HX, which are commonly used to generate O_2^-, increased the formation of oxyMb. In fact, when $K^+O_2^-$ reacted with metMb, ferrylMb, which has characteristic peaks at 548 and 582 nm (*32*), was resulted (Fig. 8A). Although SOD had no effect on the formation of ferrylMb, catalase completely blocked the conversion of metMb to ferrylMb. Essentially, the same results were obtained using XO-HX (Fig. 8B). Even when catalase was presented, neither $K^+O_2^-$ nor XO-HX led to the production of oxyMb from metMb. Evidently, only HRP-Fe^{3+}-NADH participates in the formation of oxyMb, and XO and HX are not involved in this process. These results indicate that the formation of oxyMb from metMb was not due to O_2^- or H_2O_2 by itself. It is likely that HRP-$Fe^{2+}\cdots O_2\cdots NAD^{\cdot}$ like NAD radical participated in the conversion of metMb to oxyMb induced by HRP-Fe^{3+}-NADH.

Discussion

The present study suggests that a ternary complex (HRP-$Fe^{2+}\cdots O_2\cdots NAD^{\cdot}$) plays a central role in the generation of O_2^- and $HO^{\cdot}$ during the reaction of HRP-Fe^{3+} with NADH under aerobic conditions. Immediately after the reaction with NADH under aerobic conditions, HRP-Fe^{3+} is converted to compound III. SOD strongly inhibited both the reduction of cytochrome *c* and the formation of compound III. Catalase inhibited only the generation of O_2^- and promoted the formation of compound III, indicating that compound III reacted with H_2O_2. Evidently, the production of most of the O_2^- was dependent upon H_2O_2, but the formation of compound III occurred independently of H_2O_2. Compound III seems to be formed via a reaction that generates O_2^- and is not inhibited by catalase. Under anaerobic conditions, the formation of ferroperoxidase was not observed. These results suggest that compound III may be produced via the formation of ternary complex consisting of HRP-Fe^{3+}, NADH and O_2 and that this process does not occur through the reaction of ferroperoxidase with O_2.

It has previously been shown that compound III is formed through the direct reaction of peroxidase with O_2^- (*33–37*). Indeed, O_2^- generated by XO-HX caused the conversion of HRP-Fe^{3+} to compound III. However, it is unlikely that most of the formation of compound III was due to O_2^- because even when the generation of O_2^- was strongly inhibited by catalase, the formation of compound III occurred. As a result, the contribution of O_2^- to the formation of compound III may therefore have been quite small.

Afanasyeva *et al.* (*4*) suggested a pathway that begins one electron transfer from NADH to HRP-Fe^{3+} to form the NAD radical and compound III. Formation of O_2^-, which was produced during the formation of compound III, should thus be closely correlated with the generation of the NAD radical. However, compound III was formed concomitantly with the generation of O_2^- through interaction of HRP-Fe^{3+} and NADH with O_2. Recognizable spectral change did not occur during the reaction of HRP-Fe^{3+} with NADH under anaerobic conditions. Therefore, it appears that a ternary complex consisting of HRP-$Fe^{2+}\cdots O_2\cdots NAD^{\cdot}$ participates in the generation of O_2^- and the formation of compound III. These processes were illustrated in Fig. 9.

Firstly, oxygen may be fixed between NADH and ferric iron in the haem of HRP. One electron may then be transferred from NADH to O_2, and then O_2 can subsequently be reduced to O_2^-. The O_2^- may transfer to the haem of HRP, thus leading to its conversion to compound III (HRP-$Fe^{2+}O_2$). Another O_2 may be incorporated between the NAD radical and the haem in compound III, thus resulting in the production of O_2^-, NAD^+ and compound III.

The generation of hydroxyl radicals is found to be dependent upon O_2^- and H_2O_2 because SOD and catalase inhibited the formation of $HO^{\cdot}$. However, it is unlikely that the $HO^{\cdot}$ are formed from H_2O_2 and O_2^- by the iron-catalyzed Haber–Weiss reaction because even small traces of iron in the buffer used in this

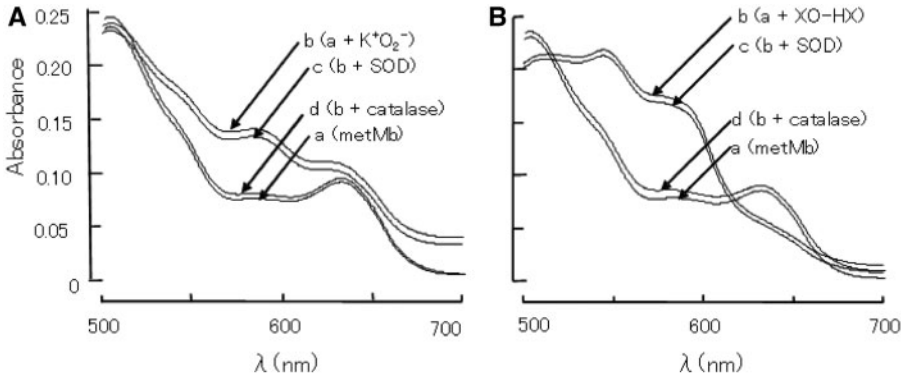

Fig. 8 Oxidation of metMb by $K^+O_2^-$ (A) and XO-HX (B). Experimental conditions were the same as described in Fig.6 except for the addition of HRP-Fe^{3+}-NADH. In (A) $K^+O_2^-$ (10 mM) was added to the reaction mixture. After the incubation for 1 min, the spectra of Mb were recorded. Curve a, metMb; curve b, curve a + $K^+O_2^-$; curve c, curve b + SOD (3 μM); and curve d, curve b + catalase (0.4 μM). In (B), XO (0.025 u/ml)-HX (0.1 mM) was added to the reaction mixture. After the incubation for 5 min, the spectra of Mb were recorded. Curve a, metMb; curve b, curve a + XO-HX; curve c, curve b + SOD (3 μM); and curve d, curve b + catalase (0.4 μM).

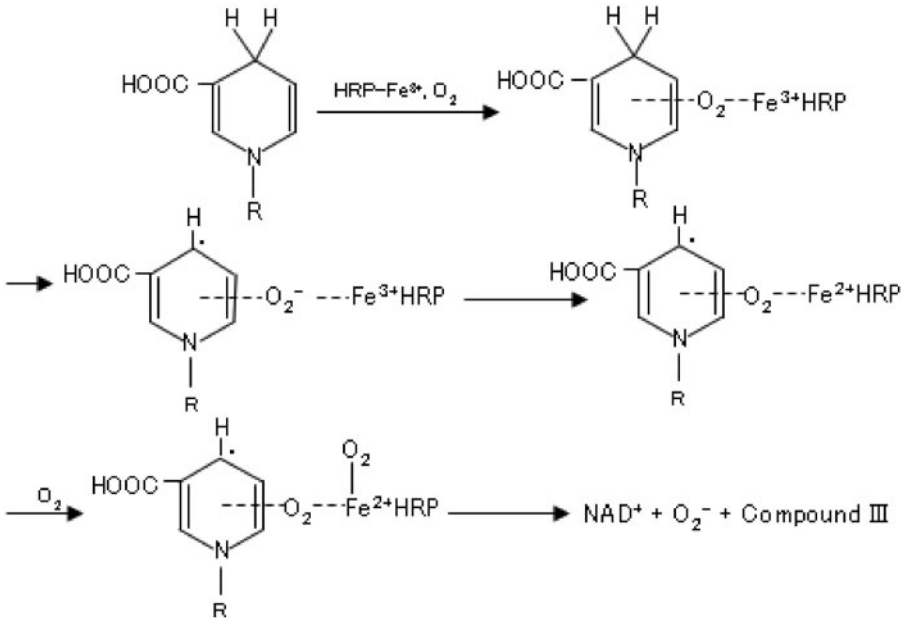

Fig. 9 The mechanism by which the generation of O_2^- is induced by HRP-Fe^{3+}-NADH.

study are removed by chelex-100, and DTPA, which is an inhibitor of Haber–Weiss reaction (*38*). Further demonstrating this fact, the ESR signal for $HO^{\cdot}$ was not observed during the reaction of $K^+O_2^-$ with H_2O_2 (data not shown).

Chen and Schopfer (13) suggest that compound III catalyzes the formation of $HO^{\cdot}$ during the reaction with H_2O_2. In the present study, the formation of $HO^{\cdot}$ was dependent upon the concentrations of HRP-Fe^{3+} and NADH. However, I note that H_2O_2 caused changes in the spectrum of compound III to compound II without any enhancement of the formation of $HO^{\cdot}$.

MetMb was converted to oxyMb during the reaction of HRP-Fe^{3+} with NADH. SOD and catalase strongly inhibited the formation of oxyMb. In contrast, $K^+O_2^-$ or XO-HX did not induce the formation of oxyMb. It was therefore concluded that the formation of oxyMb from metMb was not due to free O_2^- or H_2O_2 itself. It is known that $HO^{\cdot}$ is generated from the reaction of a semiquinone radical with H_2O_2 via a non-Haber–Weiss reaction (*39*). The chemical structure of the NAD radical is similar to a semiquinone. It can be inferred that if the properties of the NAD radical are similar to those of semiquinone radicals, $HO^{\cdot}$ may be generated via the non-Haber–Weiss reaction as follows:

$$NAD\cdot + H_2O_2 \rightarrow NAD^+ + HO\cdot + OH^- \qquad (3)$$

However, it is unlikely that the process represented in equation (1) contributed to $HO^{\cdot}$ formation by HRP-Fe^{3+}-NADH, because if this was the case, SOD should not inhibit the formation of $HO^{\cdot}$ from

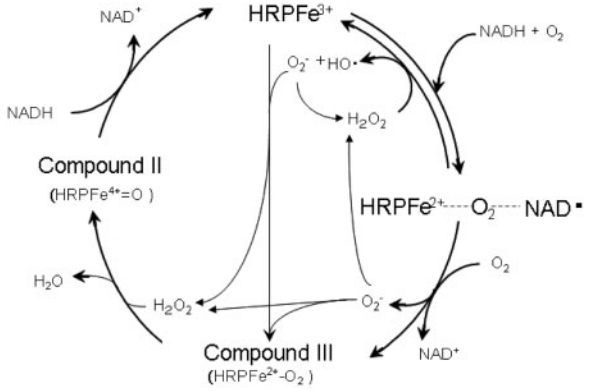

Fig. 10 HRP-Fe^{3+}-compound III cycling in the presence of NADH.

HRP-Fe^{3+}-NADH. Under aerobic conditions, semiquinones can reduce metMb, while SOD inhibits the reduction of methemoglobin (*40*). These findings strongly suggest that a ternary complex consisting of HRP-$Fe^{2+}\cdots O_2\cdots NAD\cdot$ like the NAD radical plays a central role in the formation of $HO\cdot$, the production of oxyMb from metMb and the reduction of O_2. Hydroxyl radicals, O_2^- and oxyMb may be produced through the reaction of the ternary complex with H_2O_2, O_2 and metMb, respectively, as follows in equations (4) to (6):

$$\mathrm{HRP-Fe^{2+}\cdots O_2\cdots NAD\cdot + H_2O_2 \rightarrow HO\cdot + O_2^- + NAD^+ + HRP-Fe^{3+}} \quad (4)$$

$$\mathrm{HRP-Fe^{2+}\cdots O_2\cdots NAD\cdot + O_2 \rightarrow O_2^- + compound\ III + NAD^+} \quad (5)$$

$$\mathrm{HRP-Fe^{2+}\cdots O_2\cdots NAD\cdot + O_2 + metMb \rightarrow oxyMb + NAD^+ + compound\ III} \quad (6)$$

The overall reaction of HRP-Fe^{3+} with NADH is shown in Fig. 10 in which a cyclic pathway may be formed between HRP-Fe^{3+}, compound III and compound II in the presence of NADH under aerobic conditions. Superoxide may only partially contribute to the formation of compound III and most of them may dismutate to H_2O_2 as follows:

$$\mathrm{HRP-Fe^{3+} + O_2^- \rightarrow compound\ III} \quad (7)$$

$$2O_2^- + 2H^+ \rightarrow H_2O_2 + O_2 \quad (8)$$

SOD and catalase inhibit the cyclic pathway through preventing of the formation of the HRP-$Fe^{2+}\cdots O_2\cdots NAD\cdot$ or blocking the reaction with the HRP-$Fe^{2+}\cdots O_2\cdots NAD\cdot$ by scavenging O_2^- and H_2O_2.

Although I did not investigate their importance during the present study, other peroxidases such as lactoperoxidase and myeloperoxidase also produced $HO\cdot$ in the presence of NADH. Winterbourn (*41*) demonstrated that myeloperoxidase acted as an effective inhibitor to $HO\cdot$ produced from XO-HX in the presence of Fe^{3+}-EDTA through the breakdown of H_2O_2. In the system, myeloperoxidase blocks the generation of $HO\cdot$ by scavenging O_2^-. However, the present data indicated that HRP-Fe^{3+} was converted to compound III with the generation of O_2^- in the presence of NADH. The ability to generate $HO\cdot$ is different between peroxidases (*13*).

Funding

This work was supported by the Research Fund of Hokkaido Shoushi Gakuen.

Conflict of interest

None declared.

References

1. Prasad, T.K., Anderson, M.D., Martin, B.A., and Stewart, C.R. (1994) Evidence for chilling-induced oxidative stress in maize seedlings and a regulatory role for hydrogen peroxide. *Plant Cell* **6**, 65–74
2. George, P. (1953) The chemical nature of the second hydrogen peroxide compound formed by cytochrome c peroxidase and horseradish peroxidase. I. Titration with reducing agents. *Biochem. J.* **54**, 267–276
3. George, P. (1953) The chemical nature of the second hydrogen peroxide compound formed by cytochrome c peroxidase and horseradish peroxidase. 2. Formation and decomposition. *Biochem. J.* **55**, 220–230
4. Afanasyeva, M.S., Taraban, M.B., Purtov, P.A., Leshina, T.V., and Grissom, C.B. (2006) Magnetic spin effects in enzymatic reactions: radical oxidation of NADH by horseradish peroxidase. *J. Am. Chem. Soc.* **128**, 8651–8658
5. Kirkor, E.S. and Scheeline, A. (2000) Nicotinamide adenine dinucleotide species in the horseradish peroxidase-oxidase oscillator. *Eur. J. Biochem.* **267**, 5014–5022
6. Yokota, K. and Yamazaki, I. (1977) Analysis and computer simulation of aerobic oxidation of reduced nicotinamide adenine dinucleotide catalyzed by horseradish peroxidase. *Biochemistry* **16**, 1913–1920
7. Yamazaki, I. and Yokota, K. (1965) Conversion of ferrous peroxidase in to compound III in the presence of NADH. *Biochem. Biophys. Res. Commun.* **19**, 249–254
8. Dordick, J.S., Klibanov, A.M., and Marletta, M.A. (1986) Horseradish peroxidase catalyzed hydroxylations: mechanistic studies. *Biochemistry* **25**, 2946–2951
9. Jenzer, H., Kohler, H., and Broger, C. (1987) The role of hydroxyl radicals in irreversible inactivation of lactoperoxidase by excess H_2O_2; A spin-trapping/ESR and absorption spectroscopy study. *Arch. Biochem. Biophys.* **258**, 381–390
10. Halliwell, B. (1977) Generation of hydrogen peroxide, superoxide and hydroxyl radicals during the oxidation of dihydroxyfumaric acid by peroxidase. *Biochem. J.* **163**, 441–448
11. Schweikert, C., Liszkay, A., and Schopfer, P. (2000) Scission of polysaccharides by peroxidase-generated hydroxyl radicals. *Phytochemistry* **53**, 565–570
12. Schweikert, C., Liszkay, A., and Schopfer, P. (2002) Polysaccharide degradation by Fenton reaction- or peroxidase-generated hydroxyl radicals in isolated plant cell walls. *Phytochemistry* **61**, 31–35

13. Chen, S.X. and Schopfer, P. (1999) Hydroxyl-radical production in physiological reactions. A novel function of peroxidase. *Eur. J. Biochem.* **260**, 726–735
14. Fujimoto, S., Kawakami, N., and Ohara, A. (1993) Formation of a hydroxyl radical by the myeloperoxidase-NADH-oxygen system. *Biol. Pharm. Bull.* **16**, 525–528
15. Kawakami, N., Hayakawa, T., Shimohama, S., and Fujimoto, S. (1993) The hydroxyl radical formation system in polymorphonuclear leukocytes. *Biol. Pharm. Bull.* **22**, 1034–1037
16. Fujimoto, S., Ishimitsu, S., Hirayama, S., Kawakami, N., and Ohara, A. (1991) Hydroxylation of phenylalanine by myeloperoxidase-hydrogen peroxide system. *Chem. Pharm. Bull.* **39**, 1598–1600
17. Babior, B.M., Kipnes, R.S., and Curnutte, J.T. (1973) Biological defense mechanisms. The production by leukocytes of superoxide, a potential bactericidal agent. *J. Clin. Invest.* **52**, 741–744
18. Johnston, R.B. Jr, Keele, B.B. Jr, Misra, H.P., Lehmeyer, J.E., Webb, L.S., Baehner, R.L., and Rajagopalan, K.V. (1975) The role of superoxide anion generation in phagocytic bactericidal activity. Studies with normal and chronic granulomatous disease leukocytes. *J. Clin. Invest.* **55**, 1357–1372
19. Cohen, H.J., Newburger, P.E., Chovaniec, M.E., Whitin, J.C., and Simons, E.R. (1981) Opsonized zymosan-stimulated granulocytes-activation and activity of the superoxide-generating system and membrane potential changes. *Blood* **58**, 975–982
20. Gutteridge, J.M., Maidt, L., and Poyer, L. (1990) Superoxide dismutase and Fenton chemistry. Reaction of ferric-EDTA complex and ferric-bipyridyl complex with hydrogen peroxide without the apparent formation of iron(II). *Biochem. J.* **269**, 169–174
21. Winterbourn, C.C. (1987) The ability of scavengers to distinguish OH. production in the iron-catalyzed Haber-Weiss reaction: comparison of four assays for OH. *Free Radic. Biol. Med.* **3**, 33–39
22. Klebanoff, S.J. (2005) Myeloperoxidase: friend and foe. *Leukoc. Biol.* **77**, 598–625
23. Ramos, C.L., Pou, S., and Rosen, G.M. (1995) Effect of anti-inflammatory drugs on myeloperoxidase-dependent hydroxyl radical generation by human neutrophils. *Biochem. Pharmacol.* **49**, 1079–1084
24. Weiss, S.J. (1989) Tissue destruction by neutrophils. *N. Engl. J. Med.* **320**, 365–376
25. Clifford, D.P. and Repine, J.E. (1982) Hydrogen peroxide mediated killing of bacteria. *Mol. Cell. Biochem.* **49**, 143–149
26. Forman, H.J. and Thomas, M.J. (1986) Oxidant production and bactericidal activity of phagocytes. *Annu. Rev. Physiol.* **48**, 669–680
27. Dorris, M. and Doerge, D.R. (1994) Evidence for a radical mechanism in peroxidase-catalyzed coupling. I. Steady-state experiments with various peroxidases. *Arch. Biochem. Biophys.* **315**, 82–89
28. Das, D., Bandyopadhyay, D., and Banerjee, R.K. (1998) Oxidative inactivation of gastric peroxidase by site-specific generation of hydroxyl radical and its role in stress-induced gastric ulceration. *Free Radic. Biol. Med.* **24**, 460–469
29. Muraoka, S. and Miura, T. (2004) Inhibition of xanthine oxidase by phytic acid and its antioxidative action. *Life Sci.* **74**, 1691–1700
30. McCord, J. and Fridovich, I. (1969) Superoxide dismutase. *J. Biol. Chem.* **244**, 6040–6055
31. Ramos, C.L., Pou, S., Britigan, B.E., Cohen, M.S., and Rosen, G.M. (1992) Spin trapping evidence for myeloperoxidase-dependent hydroxyl radical formation by human neutrophils and monocytes. *J. Biol. Chem.* **267**, 8307–8312
32. Yusa, K. and Shikama, K. (1987) Oxidation of oxymyoglobin to metmyoglobin with hydrogen peroxide: involvement of ferryl intermediate. *Biochemistry* **26**, 6684–6688
33. Kobayashi, K., Hayashi, K., and Swallow, A.J. (1990) Reactions of the NAD radical with higher oxidation states of horseradish peroxidase. *Biochemistry* **29**, 2080–2084
34. Shimizu, N., Kobayashi, K., and Hayashi, K. (1989) Kinetics of the reaction of superoxide anion with ferric horseradish peroxidase. *Biochim. Biophys. Acta.* **995**, 133–137
35. Kettle, A.J., Anderson, R.F., Hampton, M.B., and Winterbourn, C.C. (2007) Reactions of superoxide with myeloperoxidase. *Biochemistry* **46**, 4888–4897
36. Metodiewa, D. and Dunford, H.B. (1989) The reactions of horseradish peroxidase, lactoperoxidase, and myeloperoxidase with enzymatically generated superoxide. *Arch. Biochem. Biophys.* **272**, 245–253
37. Cuperus, R.A., Muijsers, A.O., and Wever, R. (1986) The superoxide dismutase activity of myeloperoxidase; formation of compound III. *Biochim. Biophys. Acta* **871**, 78–84
38. Yamazaki, I. and Piette, L.H. (1990) ESR spin-trapping studies on the reaction of Fe^{2+} ions with H_2O_2-reactive species in oxygen toxicity in biology. *J. Biol. Chem.* **65**, 13589–13594
39. Bates, D.A. and Winterbourn, C.C. (1982) Deoxyribose breakdown by the adriamycin semiquinone and H_2O_2: evidence for hydroxyl radical participation. *FEBS Lett.* **145**, 137–142
40. Winterbourn, C.C., French, J.K., and Claridge, R.F. (1978) Superoxide dismutase as an inhibitor of reactions of semiquinone radicals. *FEBS Lett.* **94**, 269–272
41. Winterbourn, C.C. (1986) Myeloperoxidase as an effective inhibitor of hydroxyl radical production. Implications for the oxidative reactions of neutrophils. *J. Clin. Invest.* **78**, 545–550